SolarPACES 2024, 30th International Conference on Concentrating Solar Power, Thermal, and Chemical Energy Systems

Receivers and Heat Transfer Media and Transport: Point Focus Systems

https://doi.org/10.52825/solarpaces.v3i.2381

Published: 25 Nov. 2025

Inverse Heat Transfer Analysis for Estimating Heat Flux in Solar Tower Receivers

Vahid Safari[1,*], María Fernandez-Torrijos[1], Antonio Acosta-Iborra[1], and Celia Sobrino[1]

[1]Department of Thermal and Fluids Engineering, Universidad Carlos III de Madrid, Spain

*Correspondence: Vahid Safari, vsafari@ing.uc3m.es

Abstract. Solar power tower plants are utilized to harness solar radiation for large-scale electricity generation. The concentrated solar radiation is absorbed by the central receiver to heat a transfer fluid, which is typically a mixture of 60% sodium nitrate ($NaNO_3$) and 40% potassium nitrate (KNO_3) to temperatures up to 565°C. Extreme conditions, including high temperatures and variable heat flux, are experienced by these central receivers, necessitating precise thermal measurements to optimize energy production and maintain efficiency. In this paper, an in-house code based on an inverse analysis technique is developed to determine the absorbed heat flux on the surface of the concentrated solar power (CSP) receiver tube, using surface temperature measurements as input. It is found that a single temperature measurement from the frontal part of the tube ($0 \leq \theta < 90°$) is sufficient for the estimation of the absorbed flux within an acceptable deviation. Additionally, noise is incorporated into the input temperature data to evaluate the reliability of the code under fluctuating conditions typical of real-world applications. The effectiveness of the code in this scenario is demonstrated, reinforcing its potential for practical applications.

Keywords: Inverse Heat Conduction Problem, Solar Tower Receivers, Heat Flux Estimation

1. Introduction

Concentrated Solar Power (CSP) plants play a critical role in advancing renewable energy infrastructure. Among the different receiver configurations, central receiver systems stand out for their ability to operate at higher temperatures. These systems employ a tubular receiver design that captures intense solar radiation, typically ranging from 300 to 1000 suns, and efficiently transfers the absorbed thermal energy to a heat transfer fluid. Accurately determining the absorbed heat flux on receiver tube surfaces is crucial for optimizing the performance of concentrating solar power systems [1]. While direct heat flux measurements are ideal, they pose significant challenges in tubular receiver systems due to the extreme operating conditions, such as high temperatures, non-uniform irradiation, and the curvature of the tubes [2]. These factors complicate sensor placement, durability, and data accuracy, necessitating the use of indirect methods or advanced modeling techniques to estimate the absorbed heat flux with acceptable precision. Consequently, computational methods, particularly inverse heat conduction analysis, have emerged as valuable tools for estimating heat flux profiles [3,4]. The strength of inverse analysis lies in its ability to estimate parameters that are difficult or impossible to measure directly, making it particularly valuable for characterizing heat transfer phenomena in complex systems like tubular receivers. Unlike traditional direct heat conduction problems, where boundary heat fluxes are known and temperature distributions are calculated,

inverse heat conduction analysis utilizes surface temperature measurements to determine unknown boundary conditions. This iterative process involves refining model parameters until the predicted temperatures closely match the input observed data.

2. Numerical model

The numerical model utilized in this study is based on the inverse method, which comprises several key components [5]. Initially, the direct problem involves solving the heat conduction equation with known parameters to predict temperature distributions. In contrast, the inverse problem aims to infer unknown parameters, such as heat flux, from measured temperature data. A critical component of the inverse analysis is sensitivity analysis [6] , which assesses how variations in parameters influence the output, thereby guiding the optimization process. To enhance the accuracy of the model, the conjugate gradient method [7] is frequently employed due to its efficiency in minimizing discrepancies between predicted and observed data through iterative adjustments. An in-house MATLAB [8] code was developed using the inverse analysis method to estimate the heat flux of a solar tower receiver tube based on temperature measurements taken at various positions. The benchmark data, which served as input for the code, consisted of temperature readings at different circumferential locations obtained from Computational Fluid Dynamics (CFD) simulations conducted using ANSYS Fluent [9].

2.1 Direct problem

A transient 2D numerical model was developed, which represents a cross-section of the receiver tube. For simplicity, heat transfer along the tube axial direction was neglected, which is justified by experimental evidence showing negligible temperature gradients along the flow direction due to high mass flow rate [2] and the bulk temperature of molten salt in the cross-section is assumed to be quasi-stationary on account of the large salt flow rate. The heat exchange between the molten salt and the pipe wall was assessed using Petukhov's correlation [10]. Consequently, heat transfer by conduction occurs in the radial and circumferential directions along the pipe, following the heat diffusion equation:

$$\rho C_{\mathrm{p}} \frac{\partial T(r,\theta,t)}{\partial t} = k\left(\frac{1}{r}\frac{\partial}{\partial r}\left(r\frac{\partial T(r,\theta,t)}{\partial r}\right)+\frac{1}{r^2}\frac{\partial^2 T(r,\theta,t)}{\partial \theta^2}\right) \tag{1}$$

Where *T* is the wall temperature, ρ is the wall density, C_{p} is the specific heat of the wall, and *k* is the thermal conductivity of the wall. The boundary and initial conditions for the direct problem are defined as follows:

$$-k\frac{\partial T(r,\theta,t)}{\partial r} = h_i(T_s - T(r,\theta,t)), \quad \text{at } r = r_i \tag{2}$$

$$-k\frac{\partial T(r,\theta,t)}{\partial r} = h_{\mathrm{conv+rad}}(\theta,t)(T(r,\theta,t)-T_\infty) - q_{\mathrm{inc}}(\theta,t), \quad \text{at } r = r_o \tag{3}$$

$$\frac{\partial T(r,\theta,t)}{\partial \theta} = 0, \quad \text{at } \theta = 0,\pi \tag{4}$$

$$T(r,\theta,t) = T_{\text{ini}}, \quad \text{for } t = 0 \tag{5}$$

Where r_i and r_o are the inner and outer radii of the pipe. T_s and T_∞ denote the temperatures of the molten salt and the environment. h_i refers to the convective heat transfer between the molten salt and the pipe's inner wall, while $h_{\text{conv+rad}}$ describes the combined convective and radiative heat transfer from the pipe's outer surface to the atmosphere.

$$h_{\text{conv+rad}}(\theta,t) = h_\infty + \varepsilon\sigma_r \left(\mathrm{T}(r,\theta,t) + T_\infty\right)\left(\mathrm{T}^2(r,\theta,t) + T_\infty^2\right) \tag{6}$$

The convection coefficient between the outer pipe surface and the surrounding atmosphere is denoted as h_∞, while the Stefan-Boltzmann constant is represented by σ_r, and the emissivity of the tube surface is given by ε. The convection coefficient h_∞ was computed through Churchill's correlation for horizontal cylinders [11]. For the numerical CFD simulation using ANSYS Fluent, a symmetric portion of the tube was considered (θ ∈ [0, 180°]). Steady-state conditions were assumed, and the heat flux was modeled using a cosine function, while the area not exposed to the sun received no heat flux.

$$q_{inc} = \begin{cases} q_{inc}(t).\cos(\theta) & ,\ 0 \le \theta < 90^\circ \\ 0 & ,90^\circ \le \theta \le 180^\circ \end{cases} \tag{7}$$

2.2 Inverse problem

For solving the inverse heat conduction problem, the conjugate gradient method [7] was employed, accompanied by an adjoint problem for parameter estimation. This formulation integrates the direct problem outlined in the previous section, along with the sensitivity problem [6], the adjoint problem [12], and the gradient equations. To solve the inverse problem, the unknown function q_{inc} can be parameterized using the unknown parameter $P(t)$. The objective of the inverse problem is to ascertain the unknown parameter P using measurements of wall temperature at $r = r_o$ and various circumferential locations, represented as $Y_{r=r_o,\theta=\theta_m}$. Thus, solving the inverse problem involves minimizing the following functional:

$$J[P] = \sum_{m=1}^{M_n} \int_{t=0}^{t_f} \left(T_{r=r_o,\theta=\theta_m} - Y_{r=r_o,\theta=\theta_m}\right)^2 dt \tag{8}$$

Here, M_n represents the total number of temperature measurement points, t_f denotes the total time, and $T_{r=r_o,\theta=\theta_m}$ is the numerical solution at the measurement positions, derived from the direct problem using an estimated heat flux q_{inc}^k that was previously calculated.

2.3 Conjugate gradient method

The process for identifying the unknown parameter P involves minimizing the functional $J[P]$ through the iterative use of the conjugate gradient method. At the kth iteration, P is estimated according to the specified expression:

$$P^{k+1} = P^k - \beta^k d^k \tag{9}$$

Where β^k represents the step size for the search and d^k indicates the descent direction, which can be calculated through the following expression:

$$d^k = J'[P^k] + \gamma^k d^{k-1} \tag{10}$$

In which $J'[P]$ is the gradient of equation (8) obtained through the adjoint method, which involves multiplying equation (1) by a Lagrange multiplier and integrating the resulting expression over both space and time. γ^k is the conjugation coefficient, calculated using the following expression:

$$\gamma^k = \frac{(J'[P^k])^2}{(J'[P^{k-1}])^2}, \ \gamma^0 = 0 \tag{11}$$

The step size β^k is also determined by minimizing the functional $J[P^{k+1}]$ in relation to β^k :

$$\beta^k = \frac{\sum_{m=1}^{M_n} \int_{t=0}^{t_f} \left[\left(T_{r=r_o,\theta=\theta_m}(P^k) - Y_{r=r_o,\theta=\theta_m} \right) \Delta T_{r=r_o,\theta=\theta_m}(d^k) \right] dt}{\sum_{m=1}^{M_n} \int_{t=0}^{t_f} \left[\Delta T_{r=r_o,\theta=\theta_m}(d^k) \right]^2 dt} \tag{12}$$

Where $T_{r=r_o,\theta=\theta_m}(P^k)$ represents the result of the direct problem at the specified measurement locations of $\theta = \theta_m$ based on the estimated P^k and $\Delta T_{r=r_o,\theta=\theta_m}(d^k)$ denotes the solution of the sensitivity problem at $\theta = \theta_m$ utilizing $\Delta P = d^k$.

2.4 Stop criteria

The stopping criterion is established based on the discrepancy principle, which stipulates that the procedure is terminated when the value of the functional becomes less than the variance of the measurement errors.

$$J[P] < M_n \sigma^2 t_f \tag{13}$$

Where M_n represents the total number of temperature measurement points, and σ denotes the standard deviation of the measurement errors.

3. Results and discussion

3.1 ANSYS simulation result

Figure 1 illustrates the heat flux (a), and temperature (b) contours derived from the 3D ANSYS simulation. The generated heat flux is a result of the aiming strategy for the equatorial position $(k = 3)$ during the spring equinox, with a Direct Normal Irradiance (DNI) value of 900 W / m^2 .

Molten salt, composed of 60% $NaNO_3$ and 40% KNO_3 [13], flows through the receiver tube at an inlet temperature of 290℃ and an inlet mass flow rate of 2.842 kg/s. In this study, a receiver tube with a total length of 10 meters was analyzed. As illustrated in Figure 1, the applied aiming strategy results in a concentrated heat flux at the midsection of the tube. To evaluate the model's performance under these conditions, heat flux and temperature data were extracted at the cross-section located 5.5 meters from the base of the tube, as indicated by the dashed line in Figure 1. The resulting temperature profile will be used as input data for the inverse analysis code, while the heat flux curve will serve to validate the accuracy of the predicted heat flux produced by the inverse analysis.

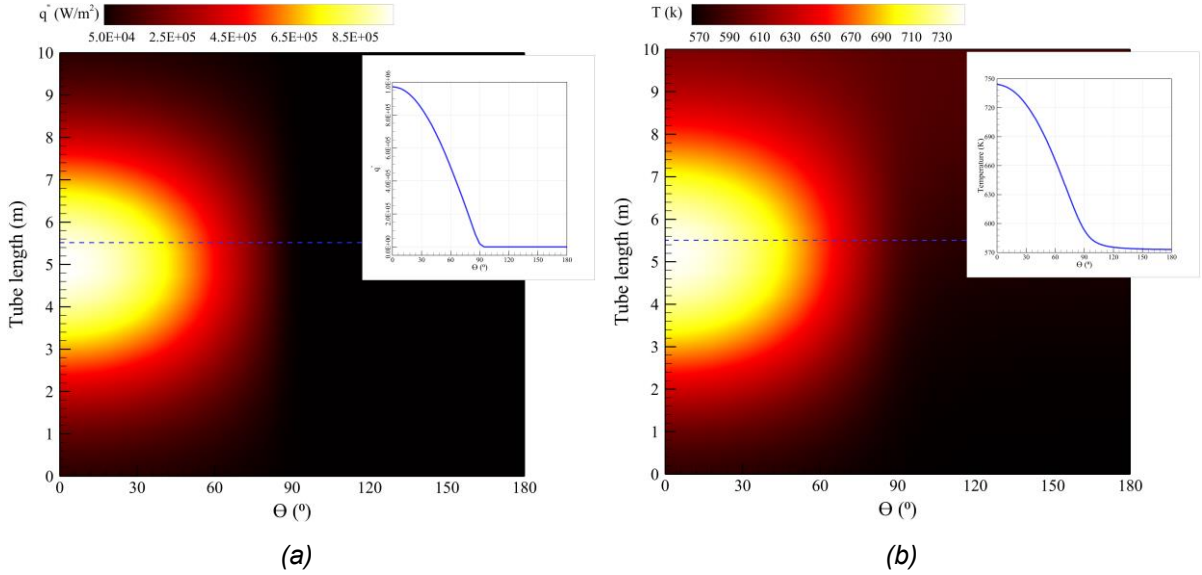

(a) *(b)*

Figure 1. *Heat flux (a), and temperature (b) contours derived from the 3D ANSYS simulation*

Figure 2 (a) presents the 2D cross-section of the tube, including the boundary conditions utilized in the inverse analysis code. Only half of the tube is simulated due to the symmetry inherent in the model. To assess the independence of the generated grid, four different mesh resolutions were tested. It was determined that a grid comprising 9 elements in the radial direction and 54 elements in the circumferential direction provided the best choices, balancing acceptable computational cost and error (Figure 2 (b)).

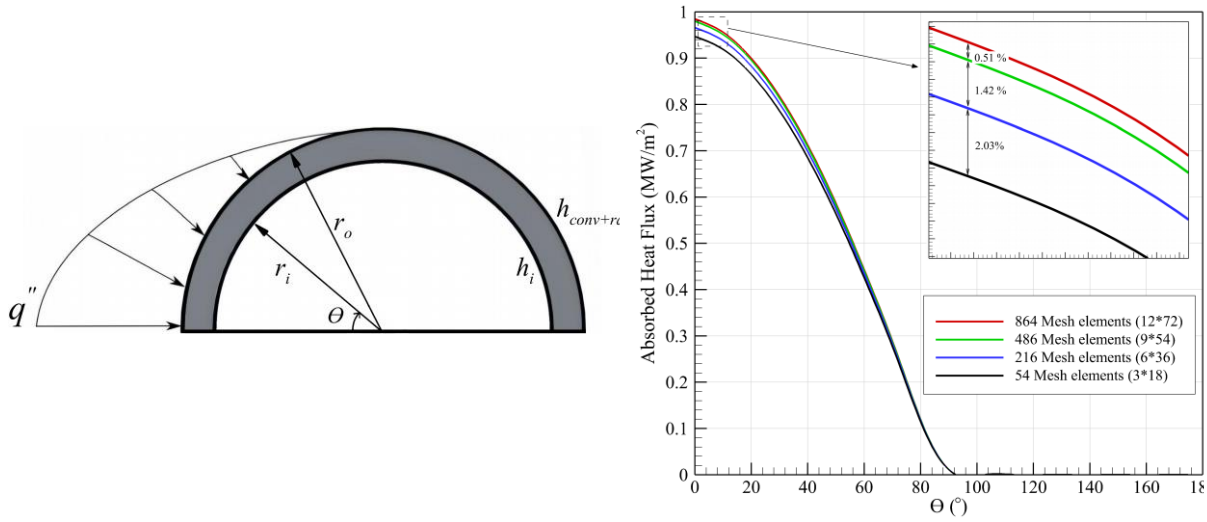

(a) *(b)*

Figure 2. *2D cross-section of the simulated domain (a) and results of the independence test (b) used in the inverse analysis code*

Figure 3(a) depicts the heat flux predictions generated by the inverse analysis code, which utilizes single-point temperature measurements from the tube's outer surface. The input temperature positions range from an angle of 10° to 100°. In the frontal region of the tube (0° ≤ θ < 90°), the optimal measurement angle is identified at 70°, resulting in the minimal deviation between the predicted heat flux and the benchmark results from ANSYS simulations, with a discrepancy of -5.01%. Across all measurement angles, the inverse analysis code consistently underestimates the heat flux compared to ANSYS results. In the rear section of the tube (90° ≤ θ ≤ 180°), only one measurement angle beyond 90°, specifically at 100°, was tested. This angle resulted in a significant discrepancy of -66.77% relative to the ANSYS reference. Attempts to use measurement angles greater than 100° led to non-convergence of the inverse analysis code.

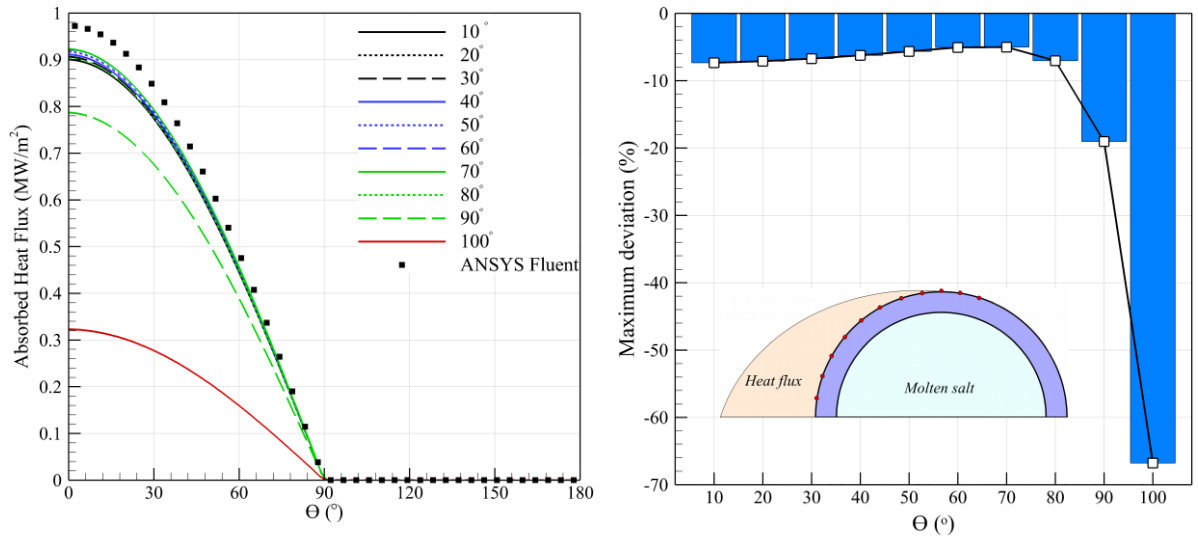

(a) *(b)*

Figure 3. *Predicted heat flux (a) and resulting deviation error (b) from the inverse analysis code*

In real-world applications, obtaining perfectly smooth data without fluctuations is nearly impossible. To assess the effectiveness of the developed inverse analysis code, a transient

stream of temperature data was augmented with white noise characterized by standard deviations of ±2, ±4, and ±6 ºC (Figure 4(a)). White noise is defined as a random signal with a constant power spectral density, resulting in unpredictable variations. As illustrated in Figure 4(b), the predicted heat flux shows only minor deviations and increases slightly with higher standard deviations. These findings highlight the robustness and reliability of the developed code in effectively handling noisy data, thereby confirming its suitability for practical applications.

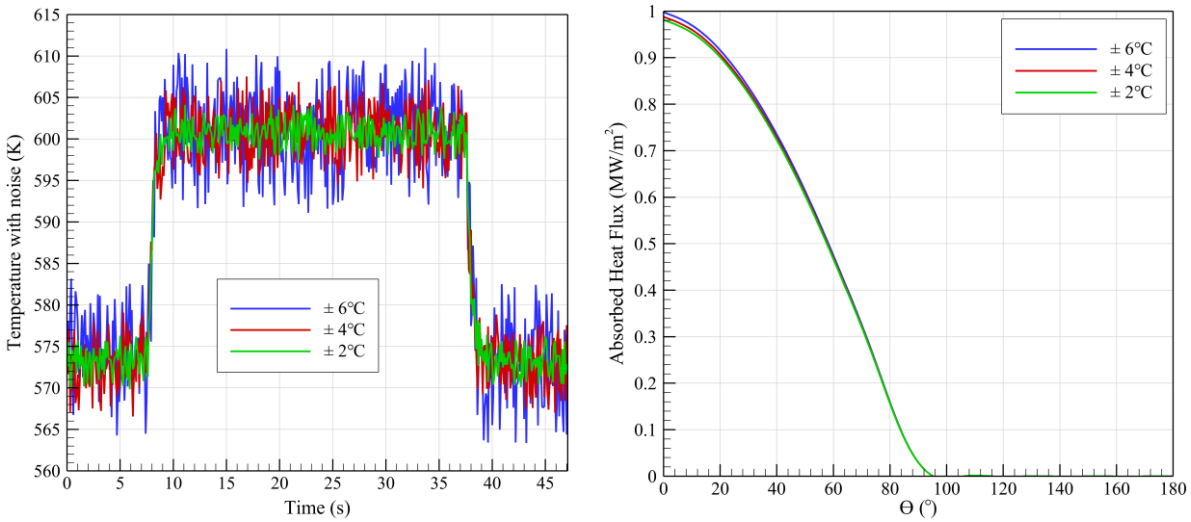

(a) *(b)*

Figure 4. *Introduced noisy temperature data (a) with the resulting heat flux prediction (b) from the inverse analysis code*

4. Conclusion

In this study, a transient 2D numerical code based on the inverse analysis method was developed to estimate the heat flux in solar tower receivers effectively. The results indicate that a single temperature measurement from the frontal section of the receiver tube can provide accurate heat flux estimations. Specifically, an optimal measurement angle of 70° yields a deviation of -5.01% compared to the benchmark results from ANSYS simulations. In contrast, predictions in the rear section of the tube exhibit significant discrepancies. Notably, at a measurement angle of 100°, the deviation reaches -66.77% relative to the ANSYS reference. The robustness of the code was further validated by incorporating noise into the temperature data, revealing that predictions remained reliable despite fluctuations. This capability underscores the method's practical applicability in real-world scenarios where data imperfections are common.

Data availability statement

Data will be made available upon request.

Author contributions

Vahid Safari: Methodology, Validation, Software, Writing – original draft, Writing – review & editing. María Fernandez-Torrijos: Supervision, Conceptualization, Methodology, Writing – review & editing. Antonio Acosta-Iborra: Supervision, Conceptualization, Methodology, Writing – review & editing. Celia Sobrino: Supervision, Conceptualization, Methodology, Writing – review & editing.

Competing interests

The authors declare that they have no known competing financial interests or personal relationships that could have appeared to influence the work reported in this paper.

Funding

This work was funded by the European Union (HORIZON MSCA Doctoral Network, Project number 101072537).

References

[1] M. Fernández-Torrijos, C. Sobrino, J.A. Almendros-Ibáñez, C. Marugán-Cruz, D. Santana, Inverse heat problem of determining unknown surface heat flux in a molten salt loop, Int. J. Heat Mass Transf. 139 (2019) 503–516. https://doi.org/10.1016/j.ijheatmasstransfer.2019.05.002.

[2] M. Fernández-Torrijos, C. Sobrino, C. Marugán-Cruz, D. Santana, Experimental and numerical study of the heat transfer process during the startup of molten salt tower receivers, Appl. Therm. Eng. 178 (2020) 115528. https://doi.org/10.1016/J.APPLTHERMALENG.2020.115528.

[3] N. Perakis, O.J. Haidn, Inverse heat transfer method applied to capacitively cooled rocket thrust chambers, Int. J. Heat Mass Transf. 131 (2019) 150–166. https://doi.org/10.1016/J.IJHEATMASSTRANSFER.2018.11.048.

[4] J. Taler, P. Duda, B. Weglowski, W. Zima, S. Gradziel, T. Sobota, D. Taler, Identification of local heat flux to membrane water-walls in steam boilers, Fuel. 88 (2009) 305–311. https://doi.org/10.1016/J.FUEL.2008.08.011.

[5] K.A. Woodbury, H. Najafi, F. Monte, J. V. Beck, Inverse Heat Conduction, Inverse Heat Conduct. (2023). https://doi.org/10.1002/9781119840220.

[6] [6]O.M. Alifanov, Inverse Heat Transfer Problems, (1994). https://doi.org/10.1007/978-3-642-76436-3.

[7] T. Lu, B. Liu, P.X. Jiang, Y.W. Zhang, H. Li, A two-dimensional inverse heat conduction problem in estimating the fluid temperature in a pipeline, Appl. Therm. Eng. 30 (2010) 1574–1579. https://doi.org/10.1016/J.APPLTHERMALENG.2010.03.011.

[8] The MathWorks Inc., 2022. MATLAB version: 9.13.0 (R2022b). Natick, Massachusetts: https://www.mathworks.com

[9] ANSYS, Inc., 2024. ANSYS Academic Research Mechanical, Release 2024 R1. Canonsburg, Pennsylvania: ANSYS, Inc. https://www.ansys.com

[10] B.S. Petukhov, Heat Transfer and Friction in Turbulent Pipe Flow with Variable Physical Properties, Adv. Heat Transf. 6 (1970) 503–564. https://doi.org/10.1016/S0065-2717(08)70153-9.

[11] S.W. Churchill, H.H.S. Chu, Correlating equations for laminar and turbulent free convection from a horizontal cylinder, Int. J. Heat Mass Transf. 18 (1975) 1049–1053. https://doi.org/10.1016/0017-9310(75)90222-7.

[12] J. Su, A.J. Silva Neto, Two-dimensional inverse heat conduction problem of source strength estimation in cylindrical rods, Appl. Math. Model. 25 (2001) 861–872. https://doi.org/10.1016/S0307-904X(01)00018-X.

[13] A.B. ZAVOICO, Solar Power Tower Design Basis Document, Revision 0, Tech. Rep. SAND2001-2100. (2001) 148. https://doi.org/10.2172/786629.